American Mineralogist, Volume 70, pages 1238–1247, 1985

Molecular mimicry of the geometry and charge density distribution of polyanions in borate minerals

Z. G. ZHANG

Department of Mathematics and Physics
Chengdu College of Geology
Chengdu 610059, Sechuan, People's Republic of China

M. B. BOISEN, JR.

Department of Mathematics
Virginia Polytechnic Institute and State University
Blacksburg, Virginia 24061

L. W. FINGER AND G. V. GIBBS

Department of Geological Sciences
Virginia Polytechnic Institute and State University
Blacksburg, Virginia 24061

Abstract

The geometries of a variety of borate polyanions extracted from borate crystals and protonated to achieve quasi-neutral or neutral molecules have been optimized using quantum mechanical molecular orbital methods. The calculated bond lengths and angles for the neutral molecules are in good agreement with those in borate minerals. However, calculations on molecules with negative charges as large as two electrostatic units yield bridging angles that depart by as much as 15° and BO bond lengths that depart by as much as 0.03Å from observed values. Even in this case, when these molecules can be neutralized by further protonation, the calculated angles agree with observed values. A regression analysis of bond strength and calculated BO bond lengths yield bond strength-bond length parameters that are identical with those obtained for crystals. Deformation electron density maps calculated for various borate molecules mimic experimental maps of comparable units in crystals; however, they fail to provide evidence for the bonding of discrete OBO units into endless chains as recently proposed for $LiBO_2$.

A reaction involving a monomer, a dimer and a 6-membered ring of triangles is examined. An analysis of the energetics of the reaction indicates that an important component of the destabilization energy of the ring is bond angle strain.

A variant on a hybrid orbital model is developed and used to rank bond lengths in distorted borate triangles and tetrahedra in crystals. One inescapable conclusion drawn in this study is that the bond lengths and angles in polyanions in borate crystals behave as if they are primarily determined by short-range forces.

Introduction

Molecular modeling of solids has been successfully used to study the physical properties of the more common rock-forming minerals. In these studies, static properties such as geometries and charge density distributions and dynamical properties such as force constants and vibrational frequencies of minerals have been calculated. In numerous cases, the results of these calculations have reproduced experimental data within the experimental error.

The premise upon which this modeling rests is that properties such as bond length and angle variations, charge density deformation distributions, etc., behave as if they are determined by short-range forces. In studying these properties, a small representative aggregate of atoms is extracted from the structure of a crystal and its static and dynamic properties are calculated using the methods of computational quantum chemistry (cf. Szabo and Ostlund, 1982). In order to mimic the crystalline environment from which the aggregate was taken, protons are added to the ends of the bonds severed in the imaginary extraction process. This makes the aggregate neutral or nearly so and models, in part, the local connectedness of the aggregate with other atoms in the crystal. The geometry of this aggregate is then

0003–004X/85/1112–1238$02.00

optimized by simultaneously varying both bond lengths and angles until the total energy of the resulting configuration is minimized and an optimal wave function for the molecule is determined. Much of the work to date has been concerned with silicates, aluminosilicates, borosilicates, thiosilicates and phoshates (Tossell and Gibbs, 1977, 1978; Newton and Gibbs, 1980; O'Keeffe et al., 1980; Gibbs et al., 1981; Newton, 1981; Gibbs, 1982; Hill et al., 1983; Ross and Meagher, 1984; Geisinger et al., 1985; O'Keeffe and Gibbs, 1984; Geisinger and Gibbs, 1981; Navrotsky et al., 1985; O'Keeffe et al., 1985). The electronic structure of the boron atom is simpler than that of silicon, and so it is reasonable to expect that the molecular modeling approach may be applicable to the borates as well.

Snyder (1978, p. 151–166), Gupta and Tossell (1981; 1983), Gupta et al., (1981), and Joyner et al., (1980) have used molecular modeling to calculate reaction energies, bond lengths and angles for borate monomers and dimers. The calculated bond lengths are in good agreement with those in crystals, but calculated bridging angles depart by as much as 10° from those observed. In this study, calculations are presented for borate triangles and tetrahedra comprising a variety of polyanions. The calculations show that both bond lengths and angles agree with observed values when completed on neutral molecules and when polarization functions are added to split valence basis sets for the bridging oxygen. A mapping of the deformation electron density of a $H_4B_2O_5$ dimer shows a spatial distribution of the bonding and lone pair electrons that is topographically similar to that recorded for a borate crystal. An analysis of the calculated reaction energy involving a six-membered ring indicates that an important component of the destabilization energy of such a structure is bond angle strain. Also, Coulson's (1961) hybridization model is adapted via an optimization procedure to calculate the fraction of *s*-character of the bonds in distorted borate triangles and tetrahedra. This study serves to advance our understanding of the crystal chemistry of the borates by showing that the forces that govern the local geometry behave as though they are primarily short-range.

Borate polyanions

Christ (1960) and Christ and Clark (1977) have shown that borates can be classified on the basis of the polymerization of BO_3 triangular (△) and BO_4 tetrahedral (T) groups into polyanions. In this scheme, the constitution of a polyanion consisting of n triangles and p tetrahedra is denoted by the symbol (n + p:n△ + pT). In modeling the bond lengths and angles in these polyanions, we optimized the geometries for various combinations of corner sharing borate triangles and tetrahedra. Drawings of these polyanions are given in Figures 1, 2 and 4. Each of these polyanions is found in one or more minerals (Christ and Clark, 1977). For example, the triangular monomer (1:△) H_3BO_3, occurs in the mineral sassolite (orthoboric acid, H_3BO_3), whereas the tetrahedral monomer (1:T) occurs in the borosilicate reedmergnerite, $NaBSi_3O_8$ (a structural analogue of low albite). The dimer polyanion $B_2O_5^{4-}$, consisting of two corner sharing triangles (2:2△), is found in suanite, $Mg_2B_2O_5$ and the dimer $B_2O_7^{8-}$, consisting of the two corner sharing tetrahedra (2:2T), is found in danburite, $CaB_2Si_2O_8$ (Phillips et al., 1974). Among the trimers, the 6-membered (3:3△) metaborate ring $B_3O_3(OH)_3$ is found in metaboric acid, HBO_2 and the $B_3O_6^{3-}$ polyanion is believed to be a major component of boron oxide glasses with alkali oxide content less than 25 mole%. The trimer $B_3O_3(OH)_5$, consisting of a ring of two triangles and a tetrahedron (3:2△ + T) occurs as an insolated unit in ameghinite, $Na[B_3O_3(OH)_4]$ whereas the trimer $B_3O_3(OH)_5^{2-}$, consisting of a ring of a triangle and two tetrahedra (3:△ + 2T), is found in meyerhofferite $Ca[B_3O_3(OH)_5]\cdot 6H_2O$.

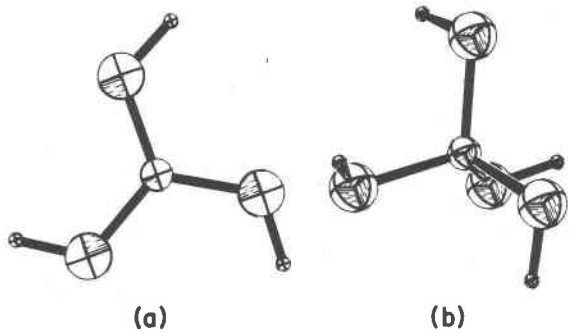

Fig. 1. Structures of borate monomers determined with near Hartree-Fock level calculations. (a) H_3BO_3 (C_1) and (b) $H_4BO_4^{1-}$ (D_{2d}). The large spheres in this figure and Figures 3 and 4 represent O and the intermediate and the small ones represent B and H, respectively. No significance is attached to the relative sizes of these spheres.

The geometry of each polyanion was optimized using an STO-3G basis set. Several were also optimized using split valence 6-31G basis sets with and without polarization functions (Binkley et al., 1980). Also, all were optimized assuming the point group indicated in Figures 1, 2 and 4. All deformation electron density maps were calculated from optimal wave functions with a 6-31G basis set augmented with polarization functions on both B and O.

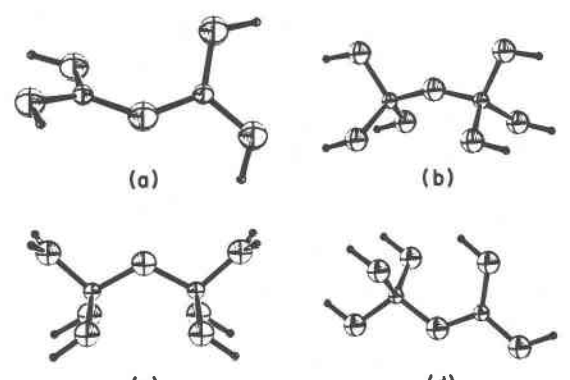

Fig. 2. Structures of borate dimers. (a) $H_4B_2O_5$ (C_2), (b) $H_6B_2O_7^{2-}$ (C_{2v}), (c) $H_8B_2O_7$ (C_{2v}), (d) $H_5B_2O_6$ (C_v).

Monomers

$H_3BO_3(1:\triangle)$

The BO bond length in the monomer H_3BO_3 has been optimized using an STO-3G basis by Gupta and Tossell (1981) (1.39Å) and by Gibbs et al., (1981) (1.37Å). These values are in agreement with the observed BO bond lengths (average R(BO) = 1.361Å) in orthoboric acid (Zachariasen, 1954) where $B(OH)_3$ molecules are linked together by hydrogen bonds. Using a split valence 4-31G basis set, Gupta and Tossell (1983) obtained a BO bond length of 1.364Å, again in agreement with the observed value. In their calculations, all OBO angles were fixed at 120° and the molecule was assumed to be planar. In our study, we optimized the geometry of $B(OH)_3$ with 11 degrees of freedom using a more robust 6-31G* basis (a 6-31G basis augmented with *d*-type polarization functions) and obtained the geometry shown in Figure 1a. All the bond lengths and angles were varied, and the molecule was allowed to be noncoplanar (C_1 point symmetry). Despite this latter degree of freedom, the optimized molecule is planar. All three of the optimized BO bonds (Table 1) in the molecule are of identical length (1.358Å) and agree to within 0.003Å of the average BO bond length in orthoboric acid. It is of interest that two of the three OBO angles in the observed structure are on average about 0.4 degrees wider than 120° whereas the third is on average 0.8 degrees narrower than 120°. This conforms with the calculated structure which shows a similar angular distribution with two angles 0.2 degrees wider and one 0.4 degrees narrower than 120°. Moreover, the angles in one of the borate groups in orthoboric acid are in exact agreement with the calculated values. The calculated BOH angles of the molecule agree to within about 1.0° of the average of those observed in orthoboric acid. The OH bond lengths calculated for the molecule are slightly longer than those observed, but this is as expected inasmuch as no correction was applied to the experimental values for thermal motion and because the delocalization of electrons between hydrogen and oxygen moves the charge density centroid toward the oxygen atom. As the symmetry of this molecule departs negligibly from C_{3h}, we optimized the geometry of H_3BO_3 assuming C_{3h} symmetry. Because the energy of this calculation is identical (Table 1) with that of the C_1 calculation, we conclude that the point symmetry of H_3BO_3 is C_{3h}.

Table 1. Comparison of optimized and experimental geometries for the monomer H_3BO_3

H_3BO_3 MONOMER (1:△)				
	R(BO)Å	R(OH)Å	<OBO°	E_T (a.u.)
OPT (3-21G*) C_1	1.377	0.962	120.0	-249.8094
OPT (6-31G) C_1	1.370	0.947	120.0	-251.0835
			120.2 (2x)	
OPT (6-31G*) C_1	1.358	0.946	119.6 (1x)	-251.1817
OPT (6-31G*) C_{3h}	1.358	0.947	120.0	-251.1817
EXP. AVE.	1.361	0.88	120.0	
EXP. RANGE	1.353-1.365	.80-.96	119.2-120.4	

$H_4BO_4^{1-}(1:T)$

In a study of the bond distances, one-electron energies and electron density distributions in first row tetrahedral hydroxy and oxyanions, Gupta et al. (1981) and Gibbs et al. (1981) optimized the BO bond length in the monomer $H_4BO_4^{1-}$ using an STO-3G basis. Despite the charge on the molecule, the calculated bond length of 1.48Å agrees with the average experimental value (1.478Å). To learn whether a 6-31G* basis calculation would yield comparable results, we optimized R(BO), R(OH), and ∠BOH assuming that the monomer had D_{2d} symmetry and identical tetrahedral OBO angles (Fig. 1b). The optimized values are R(BO) = 1.474Å, R(OH) = 0.946Å and ∠BOH = 104.0°. The average BO bond length optimized (6-31G*) for the neutral molecule H_5BO_4 is 0.02Å shorter than that for $H_4BO_4^{1-}$. The average BO bond length (1.465Å) for reedmergnerite (Appleman and Clark, 1965) agrees with that calculated for the borate monomer. In addition, O'Keeffe and Gibbs (1984) calculated the SiO bond length in monosilicic acid (1.621Å) which agrees with the average SiO bond length (1.615Å) in the borosilicate.

Dimers

$H_4B_2O_5(2:2\triangle)$

Gupta and Tossell (1983) have optimized the bridging BOB angle for the $H_4B_2O_5$ dimer assuming planar C_{2v} symmetry and fixed R(BO) = 1.379Å, R(OH) = 0.96Å and ∠OBO = 120°. The optimized angle was determined in two separate calculations using a STO-3G and a split valence 4-31G basis set, yielding bridging angles of 130 and 144 degrees, respectively. The BOB angle obtained with the STO-3G minimal basis is within 4° of the average (133.9°) angle observed for crystals (Table 2) whereas that obtained in the more robust 4-31G split valence calculation departs more than 10° from this observed value. While Gupta and Tossell only optimized the bridging angle, we completely optimized the geometry of a planar molecule using minimal (STO-3G) and split-valence 6-31G basis sets with and without polarization functions. These results (Table 2) are compared with corresponding experimental results obtained from crystals. The STO-3G results agree with the observed values quite well. However, the split valence 6-31G basis calculation (C_{2v} symmetry with 14 degrees of freedom) yielded a BOB angle that is about 10° wider than that typically observed in crystals. Adding polarization functions to the basis set for the bridging oxygen (6-31G* basis), the geometry of the $H_4B_2O_5$ dimer was optimized assuming C_{2v} symmetry. The calculation yielded bond lengths and angles that agree with observed values. This reduction of the bridging angle by addition of polarization functions to the basis set of the bridging oxygen is the same as that observed by Ernst et al. (1981) for H_6Si_2O. The more robust calculations also reproduced the tendency for $R(BO)_{br}$ to be slightly longer than $R(BO)_{nbr}$ and the tendency of $\angle O_{nbr}BO_{nbr}$ to be wider than $\angle O_{br}BO_{nbr}$ as observed in crystals with borate triangles. As the dihedral angle between the planes of adjacent triangles in diboron

Table 2. Comparison of optimized and experimental geometries for the dimer $H_4B_2O_5$

	$H_4B_2O_5$ DIMER						
	$R(BO_{br})$A	$R(BO_{nbr})$A	<BOB°	$<O_{br}BO_{nbr}$°	$<O_{nbr}BO_{nbr}$°	β	E_T (a.u.)
OPT STO-3G (C_{2v})	1.36	1.36,1.37	130.0	119.2	118.9	0	-420.6126
OPT 6-31G (C_s)	1.374	1.368	141.8	119.0,122.0	118.8	0	-426.1705
OPT 6-31G* (C_{2v})	1.368	1.364,1.350	133.4	116.8,120.9	122.3	0	-426.3418
OPT STO-3G (C_2)	1.36	1.37,1.36	129.9	119.3,121.9	118.8	9	-420.6127
OPT 3-21G* (C_2)	1.382	1.379,1.372	135.8	120.4	119.5		-424.0240
OPT 4-31G (C_2)	1.373	1.372,1.358	141.1	119.1,121.0	119.1	9	-425.7535
OPT 6-31G (C_2)	1.371	1.373,1.363	139.9	120.3,120.3	119.4	61	-426.1724
OPT 6-31G* (C_2)	1.363	1.358,1.351	131.3	119.9,120.7	119.4	58	-426.3435
EXP. AVE.	1.382	1.363	133.9	118.1	123.7		
EXP. RANGE	1.34-1.41	1.33-1.40	128-153	112-122	121-126	6-75	

trioxide varies between 5° and 75° (Gurr et al., 1970), we completely optimized the geometry of the dimer (C_2 symmetry) permitting the triangles to rotate out of the plane (Fig. 2a). The calculations were done sequentially beginning with an STO-3G basis set and followed in succession with 4-31G, 6-31G and 6-31G* basis sets. The results are given in Table 2. The diheral angles calculated using the 6-31G and 6-31G* basis sets are both about 60° falling within the range of values reported for diboron trioxide. As the energy difference between a dihedral angle of 0° and one of 60° is only 6 kJ mole^{-1}, the wide range of observed dihedral angles in B_2O_3 can be related in part to the ease with which this parameter can be distorted from its equilibrium value. This observation may also explain in part why B_2O_3 is amenable to glass formation (Gibbs, 1982; Navrotsky et al., 1985).

$H_6B_2O_7^{2-}$ and $H_8B_2O_7(2:2T)$

The $H_6B_2O_7^{2-}$ dimer consists of two borate tetrahedra each bonded to three protons (Fig. 2b). A previous optimization of this molecule by Geisinger et al. (1985) yielded a bridging angle of 134.2°, 15° wider than that of the average value in crystals. This wide angle may be ascribed in part to coulomb repulsion induced by an excess charge of 2− on the molecule. To reduce this charge and neutralize the molecule, protons were attached to two of the nonbridging oxygens of $H_6B_2O_7^{2-}$ to form the $H_8B_2O_7$ molecule shown in Figure 2c. The geometry of this dimer was optimized using an STO-3G basis with all BO bond lengths constrained to be equal (C_{2v} symmetry and 13 degrees of freedom) and with all the OBO angles fixed at 109.47°. The resulting BOB angle and BO bond lengths are 123.2° and 1.46Å, respectively, which compare well with the experimental averages of 119.0° and 1.49Å. This result is consistent with the notion that the wide angle calculated for $H_6B_2O_7^{2-}$ is due in large part to coulomb repulsions induced by the excess charge.

$H_5B_2O_6^{-1}(2:\Delta + T)$

An $H_5B_2O_6^{-1}$ dimer consisting of corner sharing BO_4 and BO_3 groups was used to model the BOB group shared between a tetrahedron and a triangle (Fig. 2d). The geometry of the molecule optimized using an STO-3G basis yielded a bridging angle of 122.8°, $R(B^{III}O) = 1.33$Å, $R(B^{IV}O) = 1.46$Å. These results compare moderately well with the experimental values of 120.5°, 1.36Å and 1.49Å, respectively, despite the charge of 1− on the molecule. The narrow range of observed bridging $B^{III}OB^{IV}$ angles (118° to 128°) between BO_3 and BO_4 groups suggests that the bending force constant of the angle is somewhat larger than that for a $B^{IV}OB^{IV}$ angle. To determine the energy required to distort the angle, we completed calculations on $H_5B_2O_6^{-1}$, varying the bridging angle from 119° to 129° but fixing the bond lengths at the optimized values. The resulting energies are plotted as a function of the angle in Figure 3 where they are compared with frequencies of observed angles taken from borates with $B^{III}OB^{IV}$ linkages. The agreement between the calculated energy curve and the histogram of the observed angles is good. The range of $B^{IV}OB^{IV}$ bridging

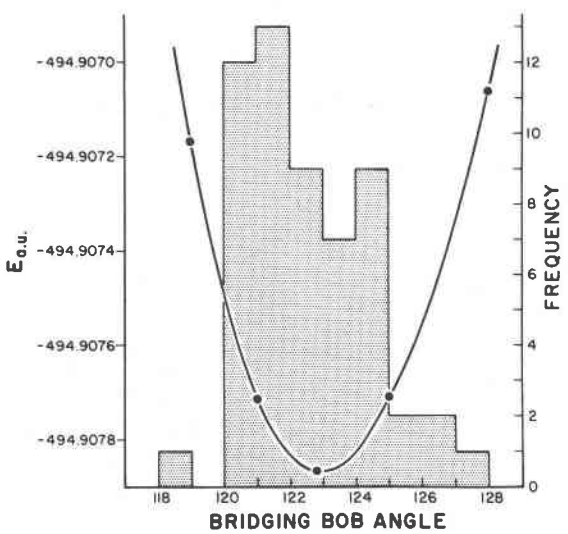

Fig. 3. Potential energy curve calculated for $H_5B_2O_6^{1-}$ as a function of the BOB angle. The histogram is a frequency distribution of the corresponding angles observed for borate crystals.

angles in borate crystals is about twice as wide (115–138°) as that for $B^{III}OB^{IV}$ (Geisinger et al., 1985) in conformity with the lesser energy required to distort the angle of a (2:2T) polyanion from its equilibrium value.

Trimers

$H_3B_3O_6(3:3\triangle)$

We optimized the geometry of $H_3B_3O_6$, a trimer consisting of a 6-membered ring of three borate triangles, using both STO-3G and a 6-31G split-valence basis sets and assuming C_{3h} symmetry (Fig. 4a). The geometry calculated with the 6-31G basis agrees well with that recorded on the average for borate crystals (Table 3). The STO-3G calculation reproduced the BO bond lengths well but reversed the order of the angles with a calculated OBO angle about 4° wider than observed. Note that the BOB angles of the trimer are more than 5° narrower than those in the $H_4B_2O_5$ dimer discussed above, suggesting that the bridging bonds are strained in the ring structure. In a determination of the magnitude of this strain energy, we considered the reaction

$$3(H_3BO_3) + H_3B_3O_6 \rightarrow 3(H_4B_2O_5). \quad (1)$$

Synder and Basch (1969) have established, for such an isodesmic reaction (where the number and type of bonds in the reacting molecules is conserved), that differences in SCF energies close to the Hartree–Fock limit give good estimates of heats of reaction. For example, O'Keeffe and Gibbs (1984) have used such energy differences to obtain estimates of the SiOSi bond angle strains in 4- and 6-membered rings in silicate molecules. More recently, O'Keeffe et al. (1985) calculated energies for the hydrolysis of TOT linkages (T = Si or P) in silicate and phosphate molecules, for hydrolysis of the monomeric metaphosphate ion and for the deprotonation energy of both phosphoric and silicic acids. For reaction (1), the calculated energy (using a 6-31G basis) for the right-hand side of the equation is 42 kJ $mole^{-1}$ lower than that for the left. The right side involves 6 unstrained BO bonds whereas the left involves 6 strained BO bonds, hence the strain energy per bond is 7 kJ $mole^{-1}$. This value is 10 kJ $mole^{-1}$ less than the strain energy per SiO bond calculated for a 6-membered ring of 4-coordinate Si atoms (O'Keefe and Gibbs, 1984). The larger strain energy for the silicate rings is consistent with the paucity of 6-membered Si_3O_6 rings in silicates and their breakdown during a trimethylsilylation reaction (Chakoumakos et al., 1981). Structures containing the 6-membered borate ring are not uncommon (Christ and Clark, 1977).

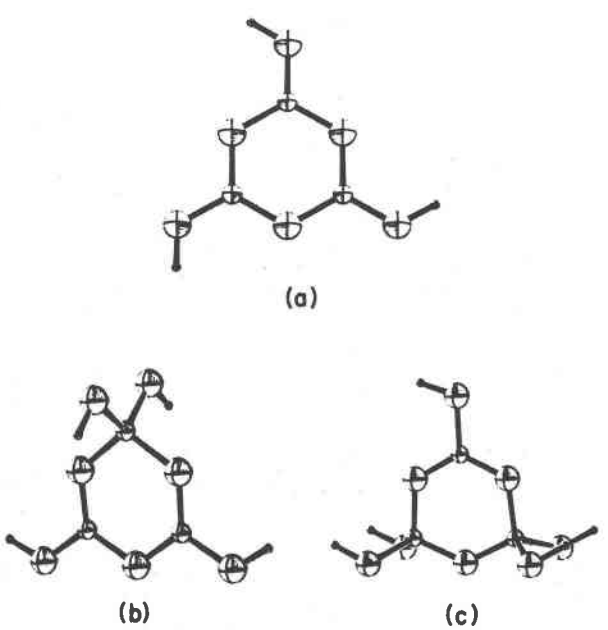

Fig. 4. Structures of borate trimers. (a) $H_3B_3O_6(C_{3h})$, (b) $H_4B_3O_7^{1-}(C_{2v})$, (c) $H_5B_3O_8^{2-}$ (C_v).

$H_4B_3O_7^{1-}(3:2\triangle + T)$

An $H_4B_3O_7^{1-}$ trimer consisting of a ring of two triangles and a tetrahedron was optimized (STO-3G) assuming C_2 symmetry (Fig. 4c). The experimental values listed (Table 3) are averaged values observed for B_3O_7 trimers in monoclinic metaboric acid (Zachariasen, 1963), biringuccite (Corazza et al., 1981) and ameghinite (Negro et al., 1975). With the exception of the OBO angles, all of the calculated bond lengths and angles fall within the range of values recorded for these solids.

$H_5B_3O_8^{2-}(3:\triangle + 2T)$

An $H_5B_3O_8^{2-}$ trimer consisting of a triangle and two tetrahedra was optimized assuming C_v symmetry (Fig. 4d). The resulting values are compared with experimental values (Table 3) taken from hydrochlorborite (Brown and Clark, 1978) and parahilgardite (Wan and Ghose, 1983). The agreement among the calculated and observed values is poorer than that for the lesser negatively charged $H_4B_3O_7^{1-}$ trimer. In particular, the calculated BOB angle between the two borate tetrahedra is 15° wider than the average observed value. As in the case of $H_6B_2O_7^{2-}$, this discrepancy may be due to its 2− charge. To correct the problem, we neutralized $H_6B_2O_7^{2-}$ by protonating two of its nonbonding oxygen atoms. Unfortunately, in the case of $H_5B_3O_8^{2-}$, we could not find satisfactory protonization sites and, therefore were unable to test this possibility with a calculation on the neutral molecule $H_7B_3O_8$.

Deformation electron density maps

The deformation density of a molecule is defined as $\Delta\rho(r) = \rho^M(r) - \rho^P(r)$ where $\rho^M(r)$ is the total molecular orbital density of the molecule and $\rho^P(r)$ is the electron density of the promolecule which is defined to consist of spherically symmetric free atoms centered at the appropriate positions in the molecule. Thus, a map of the deformation density provides an estimate of the redistribution of

Table 3. Comparison of optimized and experimental geometries for the trimers $H_3B_3O_6$, $H_4B_3O_7^{1-}$ and $H_5B_3O_8^{2-}$

$H_3B_3O_6$ TRIMER

	$R(BO_{br})$Å	$R(BO_{nbr})$Å	$BO_{br}B^\circ$	$O_{br}BO_{br}^\circ$	E_T (a.u.)
OPT STO-3G	1.37	1.35	118.8	121.2	-518.4534
OPT 6-31G	1.390	1.351	123.8	116.1	-525.2507
EXP. AVE.	1.401	1.322	122.7	117.3	
EXP. RANGE	1.373-1.433	1.280-1.355	120-125	115-120	

$H_4B_3O_7^{-1}$ TRIMER

	$R(B^{IV}O)\rightarrow B^{III}$	$R(B^{III}O)\rightarrow B^{IV}$	$R(B^{III}O)\rightarrow B^{III}$	$<B^{IV}OB^{III}$	$<B^{III}OB^{III}$	$<OB^{IV}O$	$<OB^{III}O$
OPT. STO-3G (C_{2v})	1.49	1.32	1.36	123.8	115.4	108.0	124.6
EXP. AVE.	1.478	1.353	1.387	122.5	119.9	110.9	120.7
EXP. RANGE	1.44-1.51	1.32-1.37	1.34-1.41	117-125	119-120	110-113	119-124

$H_5B_3O_8^{-2}$ TRIMER

	$R(B^{IV}O)\rightarrow B^{III}$	$R(B^{III}O)\rightarrow B^{IV}$	$R(B^{IV}O)\rightarrow B^{IV}$	$<B^{IV}OB^{III}$	$<B^{IV}OB^{IV}$	$<OB^{IV}O$	$<OB^{III}O$
OPT STO-3G (C_s)	1.48	1.33	1.45	122.0	130.6	109.5	126.5
EXP. AVE.	1.495	1.371	1.458	119.5	115.8	111.3	121.2
EXP. RANGE	1.48-1.52	1.36-1.39	1.43-1.47	113-124	115-120	110-113	121-122

the electron density that occurs when a collection of non-interacting spherically-averaged atoms is transformed into a chemically bound molecule.

If the forces that govern the charge density distribution in a crystal behave as if they are short-range and if the procrystal truely consists of spherical non-interacting atoms, then the deformation density calculated for a representative protonated aggregate of atoms extracted from a crystal should mimic the experimental density of the aggregate in the crystal. The main complication is in the choice of the basis sets used to model the atoms in the promolecule. One option followed by Gupta and Tossell (1983) is to assume that the promolecule consists of a set of spherical closed-shell ions. This approach is unsatisfactory for our purposes for the following two reasons: (1) The procrystal density is calculated using spherical atoms instead of ions (Coppens, 1982). Hence, comparisons between the deformation densities are inappropriate; and (2) deformation densities derived with a promolecule of closed shell ions subtract too much density from atoms like O and not enough from B and H. Clearly, the worst case is for H^+ which has no electrons. Thus the resulting maps in this case have a positive peak centered at the hydrogen site rather than on the OH bond.

Another option is to determine a quantum mechanical description of each of the ground state atoms using unrestricted Hartree–Fock formalism. The resulting descriptions, which are not spherical if the atom has partially filled *p* or *d* shells, must be modified to yield an atomic density matrix with the proper spherical symmetry (cf. Engel and Hagler, 1977). We have used this technique to calculate the promolecule density. By subtracting this promolecule density from the total molecular density, deformation maps were calculated for the monomer H_3BO_3, and a planar modification of the corner-sharing dimer $H_4B_2O_5$ to gain insight into the spatial distribution of the bonding and antibonding electrons in these molecules.

H_3BO_3 deformation density

The deformation map for the H_3BO_3 molecule (Fig. 5) shows peaks of bonding density in the BO (0.5 e/Å^3) and OH (0.6 e/Å^3) bonds. In addition, a larger peak of lone pair density (1.0 e/Å^3) is observed on the back side of the BOH angle. The heights and positions of the peaks on the BO bond agree with those obtained in experimental maps of $Li_3B_5O_8(OH)_2$ (Shevyrev et al., 1981) and $LiBO_2$ (Kirfel et

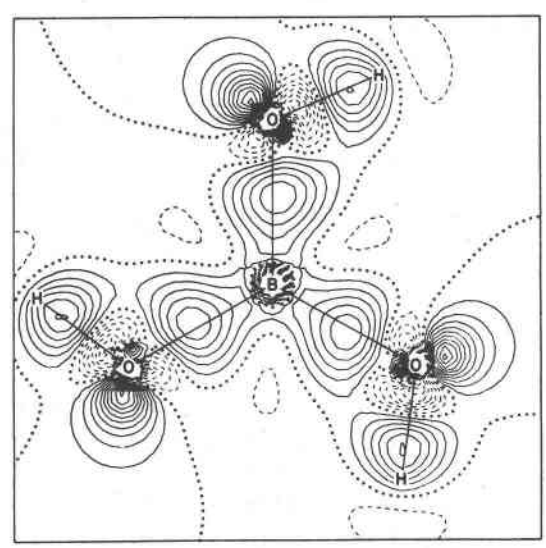

Fig. 5. Calculated charge density map for an H_3BO_3 monomer. The contour interval is 0.1 e/Å^3 with negative contours dashed and the zero level dotted. The map was calculated using a 6-31G* basis set.

al., 1983). As in the molecule, the peaks in these borates are displaced toward the more electronegative oxygen atom. Also the BO bonding peaks are displaced off the BO bond vector away from the lone pair density and toward the H atom as one might expect from simple electrostatic considerations.

$H_4B_2O_5$ deformation density

The deformation map calculated for the $H_4B_2O_5$ corner sharing dimer is compared in Figure 6 with a static map of a comparable unit in an $LiBO_2$ crystal (Kirfel et al., 1983). In the derivation of the experimental map, rigid pseudoatom multipole refinements of the borate crystal were completed with Hartree–Fock (HF) and generalized scattering factors (GSF) calculated from diatomic BO and LiO diatomic wavefunctions. Both refinements yield identical positional and thermal parameters, and the topographies of the resulting deformation maps are quite similar. As the deformation map of the monomer shows close agreement with the map derived with the Hartree–Fock formalism, we compared our results with this map. Although the maps are topographically similar, the charge density distribution of the OBO units in the two systems is different. The two peaks in the OBO unit of the monomer (Fig. 6) are not only well-developed, but they are also identical in both position and height. On the other hand, the peaks in the OBO unit of the crystal are dissimilar—one is well-developed with a peak height of 0.7 e/Å^3 and the other is lower (0.6 e/Å^3) and more diffuse. In rationalizing this difference, Kirfel et al. (1983) suggested that the chains in $LiBO_2$ are polymerized from BO_2 anions in such a way that a "free" sp^2 hybrid orbital on B can overlap with a $2p$ orbital on the bridging oxygen atom. However, the map calculated for the dimer neither shows features that may be ascribed to a "free" sp^2 hybrid on B nor evidence for a unit composed of a BO_2 anion as proposed for $LiBO_2$.

Fractional *s*-character of BO bonds in crystals

A semi-empirical molecular orbital study of the borates by Schlenker et al. (1978) has shown that wide angles tend to involve short bonds with large overlap populations for triangular and tetrahedral B oxyanions. However, their analysis did not provide a suitable model that could be applied to BO_4 groups in which the symmetry is not C_{3v}. For the general case we shall examine whether the bond lengths in borate tetrahedra and triangles in crystals of any symmetry can be ranked in terms of the fractions of *s*-character of the bonds.

Borate tetrahedra

We have applied the sp^3 hybrid model (Coulson, 1961; Bingel and Luttke, 1981) to individual tetrahedral oxyanions in borate crystals. However, because of the distortions imposed on these oxyanions by linkage factors, packing and bonding requirements, we found, as forewarned by Klahn (1983), that care must be exercised in the adaptation of this model to tetrahedra in crystals.

In the model, the hybrid orbital h_i in the ith valence direction (i = 1,2,3,4) is written as a normalized linear combination of the *s*-orbital and the p_i-orbital

$$h_i = \frac{\alpha_i s + \beta_i p_i}{\|\alpha_i s + \beta_i p_i\|}$$

where α_i and β_i are weighting coefficients for the *s*- and *p*-orbitals. Defining the hybridization parameter λ_i to be the ratio β_i/α_i, this equation becomes

$$h_i = \frac{s + \lambda_i p_i}{\|s + \lambda_i p_i\|} = \frac{s + \lambda_i p_i}{\sqrt{1 + \lambda_i^2}}$$

where $\|s + \lambda_i p_i\| = \sqrt{1 + \lambda_i^2}$ since $\{s,p_i\}$ forms an orthonormal basis set. From this equation, we find that the fraction of *s*-character of h_i is $f_i = 1/(1 + \lambda_i^2)$. Because the

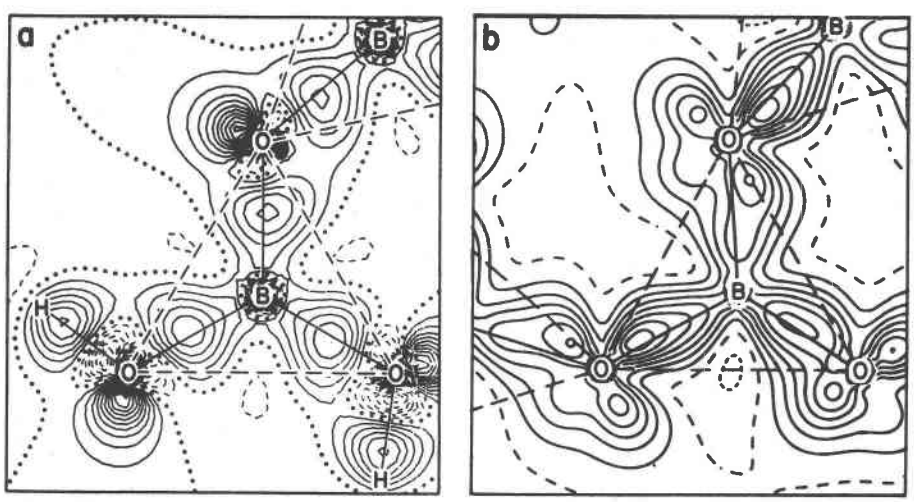

Fig. 6. Deformation density maps for corner-sharing triangles. (a) Calculated map for planar $H_4B_2O_5$ contour description is the same as in Fig. 5. (b) Experimental static deformation density map for $LiBO_2$ from Kirfel et al. (1983). The contour interval is 0.1 e/Å^3, the dashed contour is for zero and negative contours are dotted.

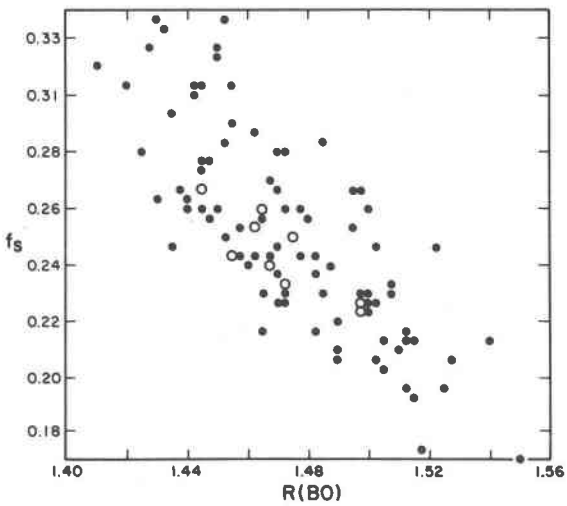

Fig. 7. A scatter diagram of observed BO bond lengths, R(BO), in borate crystals as a function of the *s*-character, f_s, of the bond. Closed circles represent single points and open circles represent two superimposed points.

hybrid orbitals are constrained to form an orthonormal set, the λ_i's are functions of the valence angles (the angles between these orbitals). The six valence angles themselves are not independent. For example, given the valence angles θ_{12}, θ_{13}, θ_{23} where θ_{ij} denotes the angle between h_i and h_j, all of the other angles and the fraction of *s*-character for each h_i can be calculated. Similarly any set of valence angles of the form θ_{ij}, θ_{ik}, θ_{jk} ($i \neq j \neq k$) can be used (Bingel and Luttke, 1981). The basic equations are of the form

$$\lambda_i^2 = -\frac{\cos\theta_{jk}}{\cos\theta_{ij}\cos\theta_{ik}}.$$

These equations together with the fact that $f_1 + f_2 + f_3 + f_4 = 1$ allow one to calculate all of the θ_{ij}'s and f_i's.

One approach in applying the hybrid orbital model to actual borate tetrahedra would be to take the angles ϕ_{ij} between the i^{th} and j^{th} BO bonds to be the valence angles. The difficulty with this approach is that if, for example, the bond angles ϕ_{12}, ϕ_{13}, ϕ_{23} are taken to be valence angles θ_{12}, θ_{13}, θ_{23}, then the other calculated valence angles θ_{14}, θ_{24}, and θ_{34} often depart from the corresponding bond angles ϕ_{14}, ϕ_{24} and ϕ_{34} by significant amounts (as much as 15°). Consequently, the calculated f_i values are unreliable. Another approach would be to repeat the process for each set of three indices {i,j,k} and average the calculated f_i values. However, the disparity in f_i values for a given i can be as great as a factor of 2 and hence this approach is also unsatisfactory. Thus, we have taken the approach of fitting to the set of bond angles the set of valence angles that are closest in terms of least squares. We then use each calculated f_i value as the fraction of *s*-character for the i^{th} bond. Using this procedure, the largest angle variation $|\theta_{ij} - \phi_{ij}|$ was found to be less than 5.5°. In a typical case, the largest angle variation is about 2.5° and the average less than 1.5°. Because of the forbidden regions for the valence angles (Klahm, 1983), a computer program was written using an approach to minimization that is designed to search within acceptable regions to find the appropriate valence angles. In Figure 7, the f_i values found for tetrahedrally coordinated boron atoms in borate crystals are plotted against the observed bond lengths. A statistical analysis shows that the linear correlation is highly significant, that 60% of the variation in the bond lengths can be explained in terms of a linear dependence on the fraction of *s*-character with shorter bonds tending to involve larger f_i values.

Borate triangles

A similar approach was taken to study the fraction of *s*-character vs. bond length variations in BO_3 groups. In the case of planar triangles, the bond angles and the valence angles can be taken to be exactly the same since the only restriction on the valence angles is that their sum be 360°. For nonplanar triangles with angles of θ_1, θ_2 and θ_3, a number k was found so that $k(\theta_1 + \theta_2 + \theta_3) = 360°$ and the valence angles were taken to be $k\theta_1$, $k\theta_2$ and $k\theta_3$, respectively. The calculation of the fraction of *s*-character f_s is then made as for the tetrahedron (Bingle and Luttke, 1981); only borate triangles without BOH bonds were considered. Regression analysis showed that the correlation is highly significant, but only 30% of the variation in bond length can be explained in terms of a linear dependency upon f_s. When triangles with BOH bonds were considered separately, the correlation between bond length is not significant at the 95% confidence level.

Discussion and conclusions

One of the most important and challenging problems in mineralogy today is the study of the forces that bond atoms together into a complex crystal structure. Progress toward understanding these forces has been made in the case of silicates, aluminosilicates, borosilicates, thiosilicates and phosphates. In these studies, it it observed that the bond lengths and angles occurring in the crystals are essentially the same as those calculated for corresponding molecular models. The close agreement between observed and calculated values presented in Figure 8 (see also Tables 1, 2

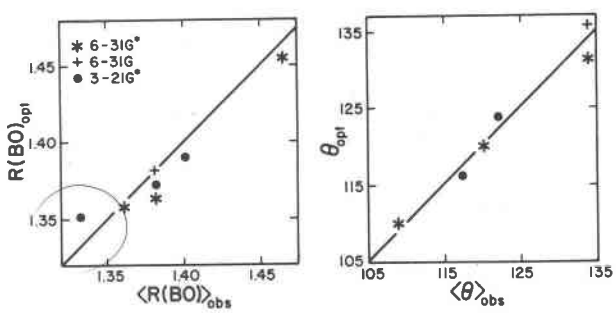

Fig. 8. A comparison of bond lengths, R(BO), and angles, θ, calculated for the neutral molecules in Figs. 1, 2 and 4 with average values observed in borate crystals. The average departure of R(BO) and θ from the 45° line is 0.01Å and 3°, respectively.

and 3) shows that the bond lengths and angles in borate crystals are also similar to those of protonated borate polyanions. In a study of bond lengths calculated for a number of hydroxyacid molecules, Gibbs (1982) showed an excellent correlation between ln(R) and ln(s) where s is the Pauling bond strength and R is the bond length. An analysis of the regression equation fit to the BO bond length data calculated in this study with split valence sets yielded the equation $s = (R(BO)/1.363)^{-3.91}$. The bond strength-bond length parameters in this equation are statistically identical with those obtained in an analysis of observed bond length-bond strength variations in more than 20 borate crystals (Brown and Shannon, 1973; Table 1). The close agreement between these two sets of parameters is evidence that the bonding forces in these crystals behave as if short-range. This is strengthened by the observation that 60% of the bond length variation of borate tetrahedra and 30% of the bond length variation of borate triangles in crystals can be ranked in terms of information obtained from the angles observed within borate polyanions. These results suggest that the bonding forces that govern the local geometry of a crystal are quite similar to those that govern the geometry of a representative molecule extracted from the crystal.

Acknowledgments

We are indebted to the National Science Foundation for supporting this study with grant EAR82-18743, to our University for providing financial support to complete the calculations described in this paper, to Virginia K. Chapman for preparing a GML version of the manuscript and to Shannon Chang for drafting several of the figures. We thank Professor E. P. Meagher of the University of Vancouver and an anonymous reviewer for providing a number of valuable observations. G. V. Gibbs wishes to thank Professor R. F. Stewart of the Chemistry Department at Carnegie Mellon University for a tutorial on the calculation of atomic wave functions for a spherically averaged charge density distributions and Professor J. A. Tossell of the Chemistry Department at the University of Maryland for a copy of the program Denmap used to calculate the deformation charge density maps reported in this paper. Z. G. Zhang wishes to express his appreciation to the Department of Geological Sciences at Virginia Tech and to Dr. G. V. Gibbs for the hospitality he received during his visit. He also wishes to thank the People's Republic of China for awarding him a Fellowship to study Quantum Mineralogy at Virginia Tech where this study was completed. Larry W. Finger wishes to thank the Carnegie Institution of Washington and the National Science Foundation (grant number EAR81-15517) for partial support during his sabbatical leave at Virginia Tech.

References

Appleman, Daniel E. and Clark, Joan R. (1965) Crystal structure of reedmergnerite, a boron albite, and its relation to feldspar crystal chemistry. American Mineralogist, 50, 1827–1849.

Bingel, Werner A. and Luttke, Wolfgang (1981) Hybrid orbitals and their applications in structural chemistry. Angewandte Chemie, 20, 11, 899–911.

Binkley, J. S., Pople, J. A. and Hehre, W. H. (1980) Self-consistent molecular orbital methods. XXI. Small split-valence basis sets for first-row elements. Journal of the American Chemical Society, 102, 939–946.

Brown, G. E. and Clark, J. R. (1978) Crystal structure of hydrochlorborite, $Ca_2[B_3O_3(OH)_4 \cdot OB(OH)_3]Cl \cdot 7H_2O$, a seasonal evaporite mineral. American Mineralogist, 63, 814–823.

Brown, I. D. and Shannon, R. D. (1973) Empirical bond-strength–bond length curves for oxides. Acta Crystallographia, A29, 266–282.

Burdett, J. K. and McLarnan, T. J. (1984) An orbital interpretation of Pauling's rules. American Mineralogist, 69, 601–621.

Chakoumakos, Bryan C., Hill, R. J. and Gibbs, G. V. (1981) A molecular orbital study of rings in silicates and siloxanes. American Mineralogist, 66, 1237–1249.

Christ, C. L. (1960) Crystal chemistry and systematic classification of hydrated borate minerals. American Mineralogist, 45, 334–340.

Christ, C. L. and Clark, J. R. (1977) A crystal-chemical classification of borate structures with emphasis on hydrated borates. Physics and Chemistry of Minerals, 2, 59–87.

Coppens, P. (1982) Concepts of charge density analysis: The experimental approach. In P. Coppens and M. Hall, Eds. Electron Distributions and The Chemical Bond, p. 61–92. Plenum Press, New York.

Corazza, Egizio, Menchetti, Silvio and Sabelli, Cesare (1974) The crystal structure of biringuccite, $Na_4[B_{10}O_{16}(OH)_2] \cdot 2H_2O$. American Mineralogist, 59, 1005–1015.

Coulson, C. A. (1961) Valence. Oxford University Press, Amen House, London.

Dal Negro, A., Martin Pozas, J. M. and Unarett, L. (1975) The crystal structure of ameghinite. American Mineralogist, 60, 879–883.

Engel, Y. M. and Hagler, A. T. (1977) Use of the Gaussian-70 molecular orbital and electron density programs. Israel Journal of Chemistry, 16, 220–225.

Ernst, C. A., Allred, A. L., Ratner, Mark A., Newton, M. D., Gibbs, G. V., Moskowitz, J. W. and Topiol, S. D. (1981) Bond angles in disiloxane: A pseudo-potential electronic structure study. Chemical Physics Letters, 81, 3.

Geisinger, K. L., Gibbs and G. V. (1981) SiSSi and SiOSi bonds in molecules and solids: A comparison. Physics and Chemistry of Minerals, 7, 204–210.

Geisinger, K. L., Gibbs, G. V. and Navrotsky, A. (1985) A molecular orbital study of bond length and angle variations in framework structures. Physics and Chemistry of Minerals, in press.

Gibbs, G. V. (1982) Molecules as models for bonding in silicates. American Mineralogist, 67, 421–450.

Gibbs, G. V., Meagher, E. P., Newton, M. D. and Swanson, D. K. (1981) A comparison of experimental and theoretical bond length and angle variations for minerals, inorganic solids, and molecules. In M. O'Keeffe, A. Navrotsky, Eds., Structure and Bonding in Crystals, 1, p. 195–225. Academic Press, New York.

Gupta, Abha and Tossell, J. A. (1981) A theoretical study of bond distances, X-ray spectra and electron density distributions in borate polyhedra. Physics and Chemistry of Minerals, 7, 159–164.

Gupta, Abha and Tossell, J. A. (1983) Quantum mechanical studies of distortions and polymerization of borate polyhedra. American Mineralogist, 68, 989–995.

Gupta, Abha, Swanson, D. K., Tossell, J. A. and Gibbs, G. V. (1981) Calculation of bond distances, one-electron energies and electron density distributions in first-row tetrahedral hydroxy oxyanions. American Mineralogist, 66, 601–609.

Gurr, G. E., Montgomery, P. W., Kuntson, C. D. and Gorres, B. T. (1970) The crystal structure of trigonal diboron trioxide. Acta Crystallographica, B26, 906–915.

Hill, R. J., Newton, M. D., and Gibbs, G. V. (1983) A crystal chemical study of stishovite. Journal of Solid State Chemistry, 47, 185–200.

Joyner, D. and Hercules, D. (1980) Chemical bonding and electronic structure of B_2O_3, H_3BO_3, and BN: An ESCA, Auger, SIMS, and SXS study. Journal of Chemical Physics, 72, 1095.

Kirfel, A., Will, G. and Stewart, R. F. (1983) The chemical bonding in lithium metaborate, $LiBO_2$. Charge densities and electrostatic properties. Acta Crystallographica, B39, 175–185.

Klahn, Bruno (1983) The relations between the valence angles of sp^3-hybridized central atoms for all possible local symmetries. Journal of Molecular Structure, 104, 49–77.

Konijnendijk, W. L. and Stevels, J. M. (1975) The structure of borate glasses studied by raman scattering. Journal of Non-Crystalline Solids, 18, 307–331.

Navrotsky, A., Geisinger, K. L., McMillan, P. and Gibbs, G. V. (1985) Implications of molecular orbital calculations on tetrahedrally bonded clusters for the structure, thermodynamics, and physical properties of glasses and melts in silicate, aluminosilicate, borosilicate, and other related systems. Physics and Chemistry of Minerals, 11, 284–298.

Newton, Marshall D. (1981) Theoretical probes of bonding in the disiloxy group. In M. O'Keeffe, A. Navrotsky, Eds., Structure and Bonding in Crystals, Vol. 1, p. 175–193. Academic Press, New York.

Newton, M. D. and Gibbs, G. V. (1980) Ab initio calculated geometries and charge distributions for H_4SiO_4 and $H_6Si_2O_7$ compared with experimental values for silicates and siloxanes. Physics and Chemistry of Minerals, 6, 221–246.

O'Keeffe, M. and Gibbs, G. V. (1984) Defects in amorphous silica; Ab initio MO calculations, Journal of Chemical Physics, 81, 876–879.

O'Keeffe, M., Newton, M. D. and Gibbs, G. V. (1980) Ab initio calculation of interatomic force constants in $H_6Si_2O_7$ and bulk modulus of α quartz and α cristobalite. Physics and Chemistry of Minerals, 6, 305–312.

O'Keeffe, M., Domenges, B. and Gibbs, G. V. (1985) Ab initio molecular orbital calculations on phosphates: Comparison with silicates. Journal of Physical Chemistry, in press.

Pauling, L. (1929) The principles determining the structure of complex ionic crystals. Journal of the American Chemical Society, 51, 1010–1026.

Phillips, M. W., Gibbs, G. V. and Ribbe, P. H. (1974) The crystal structure of danburite: A comparison with anorthite, albite, and reedmergnerite. American Mineralogist, 59, 79–85.

Ross, N. L. and Meagher, E. P. (1984) A molecular orbital study of $H_6Si_2O_7$ under simulated compression. American Mineralogist, 69, 1145–1149.

Schlenker, J. L., Griffen, D. T., Phillips, M. W. and Gibbs, G. V. (1978) A population analysis for Be and B oxyanions. Contributions of Mineralogy and Petrology, 65, 1978, 347–350.

Shevyrev, A. A., Muradyan, L. A., Simonov, V. I., Egorov-Tismenko, Y. K., Simonov, M. A. and Belov, N. V. (1981) Deformation electron density in the lithium borate $Li_3B_5O_8(OH)_2$ Soviet Physics Doklady, 26, 251–253.

Snyder, L. C. (1978) Quantum chemical calculations to model borate glass electronic structure and properties. In L. D. Pye, V. D. Frechette and N. J. Kreidl, Eds., Borate Glasses, p. 151–166. Plenum Press, New York.

Snyder, L. C. and Basch, H. (1969) Heats reaction from self-consistent field energies of closed-shell molecules. Journal of the American Chemical Society, 91, 2189–2198.

Szabo, Attila and Ostlund, Neil S. (1982) Modern quantum chemistry: Introduction to advanced structure theory. MacMillian Publishing Co., New York.

Tossell, J. A. and Gibbs, G. V. (1977) Molecular orbital studies of geometries and spectra of minerals and inorganic compounds. Physics and Chemistry of Minerals, 3, 21–57.

Tossell, J. A. and Gibbs, G. V. (1978) The use of molecular-orbital calculations on model systems for the predication of bridging-bond-angle variations in siloxanes, silicates silicon nitrides and silicon sulfides. Acta Crystallographica, A34, 463–472.

Wan, C. and Ghose, S. (1983) Parahilgardite, $Ca_6(B_5O_9)_3Cl_3 \cdot 3H_2O$: A triclinic piezoelectric zeolite-type pentaborate. American Mineralogist, 68, 604–613.

Zachariasen, W. H. (1954) The precise structure of orthoboric acid. Acta Crystallographica, 7, 305–310.

Zachariasen, W. H. (1963) The structure of cubic metaboric acid. Acta Crystallographica, 16, 380.

Manuscript received, January 4, 1985;
accepted for publication, July 24, 1985.